

Effects of simple substitutions on conformational and electronic properties of rigid rod polymer models

John W. Connolly*

Department of Chemistry, University of Missouri–Kansas City, Kansas City,
MO 64110-2499, USA

and Douglas S. Dudis

Polymer Branch, Materials Laboratory, Wright Patterson AFB, OH 45433-6533, USA
(Received 14 February 1992; revised 8 July 1992)

Conformational energies, electronic band gaps† and second-order hyperpolarizabilities were calculated as a function of torsion angle for structures designed to model the rigid rod polymers poly(*p*-phenylenebenzobisoxazole), poly(*p*-phenylenebenzobisimidazole) and poly(*p*-phenylenebenzobisthiazole), including examples in which the phenylene group is mono- and dimethylated, using AM1 semi-empirical molecular orbital techniques. An increase in torsion angle decreases π electron delocalization, which is the dominant factor in electronic band gap and second-order hyperpolarizability changes. Methylation of the phenyl group destabilizes the flat structures in all cases, and the resulting calculated barrier heights show the result of the opposing steric and conjugative effects. The methyl substituents have negligible direct effect on opto-electronic properties.

(Keywords: rigid rod polymers; substitution; conformational energy; electronic band gap; second-order hyperpolarizability; torsion angle; molecular orbitals)

INTRODUCTION

It has been recognized for some time that the rigid rod polymer poly(*p*-phenylenebenzobisoxazole) (PBO) and its sulfur analogue, poly(*p*-phenylenebenzobisthiazole) (PBZT) have exceptional specific strength and modulus, thermo-oxidative stability and environmental resistance, except for strongly acidic media, when made into films and fibres. The extreme hygroscopic nature of the NH analogue poly(*p*-phenylenebenzobisimidazole) (PBI), has limited the investigation of its properties^{1–7}.

More recently these polymers have been found to have potential as doped electrical conductors⁸. Also they have been found to display third-order nonlinear optical (NLO) properties, i.e. subpicosecond degenerate four-wave mixing measurements gave a χ^3 value of 10^{-11} esu for PBZT, with subsequent measurements on PBO giving similar results⁹.

At the molecular level, mechanical and chemical properties of these compounds are interpreted in terms of the chain stiffness as well as the molecular stability due to extensive conjugation along the polymer chain. Of course the efficiency of stacking of the polymer chains and the interaction between the chains significantly affect these properties as well. Electrical properties are related

to the electronic band gap, E_g , and the NLO properties are a function of polarizability in which π electron systems play a major role.

The molecular aspects of the above properties are amenable to treatment by computational chemical techniques. One aspect of chain stiffness is the barrier to rotation about the carbon–carbon single bonds linking the phenylene group to the aromatic heterocycle. Using a suitable model compound this barrier height can be calculated using semi-empirical molecular orbital techniques by calculation of the molecular heat of formation at each of a series of molecular conformations. Band gaps can be calculated as the difference between the frontier orbital energies in suitable model compounds. Molecular polarization can also be estimated by calculating incremental changes in molecular properties caused by a changing external electrical field using either *ab initio* or semi-empirical molecular orbital techniques¹⁰.

PBO, PBZT and PBI are soluble only in strong acid solvents, which makes processing of the fibres and films made from these rigid rod polymers difficult. Attempts to improve solubility in aprotic solvents have included synthesis of polymer analogues with pendant phenyl, benzothiazole, phenylbenzothiazole and methyl groups attached to the polymer backbone^{1,11–13}. A molecular mechanics computational study on the effect of some of the larger pendant groups has been published¹⁴. In this paper we report an extensive series of calculations in which we estimate the effect of pendant methyl and dimethyl substitutions on the barrier to phenylene

* To whom correspondence should be addressed

† Band gaps here are calculated as frontier orbital energy differences in the *model structures*, as indicated in the text. True band gaps would be for the infinite polymer

rotation in the PBO, PBZT and PBI polymer chains. Also we examine the effect of these substitutions on the electronic band gaps and we show that these substitutions have no effect on the second-order hyperpolarizabilities of these polymers.

COMPUTATIONAL DETAILS

Heat of formation and electron band gap calculations reported here were done using Version 2.1 of AMPAC including the newly-introduced sulfur parameters^{15,16} on the VAX 6460 computer at the University of Missouri–Kansas City. Specifically, the heat of formation was calculated for each structure and the conformational energy is represented normalized to the energy of the most stable conformation. Unless otherwise noted, a 0° conformation has the central phenyl ring and both of the heterocyclic species coplanar. Structures were fully optimized with the exception that the central phenyl group was constrained to be flat and the attached hydrogen atoms were constrained to be in the phenyl plane. The constraint on the phenyl hydrogen atoms was found to be without effect in several test cases.

Second-order hyperpolarizabilities were calculated using the finite field (derivative) method as implemented by the keyword POLAR in the MOPAC¹⁷ package. The default electric field increment was used.

RESULTS AND DISCUSSION

Torsional barrier calculations

Figure 1 shows two model compounds on which barrier height calculations for PBO, PBZT and, in one case, PBI have been recently reported^{14,18,19}. In both cases heats of formation were calculated at 10° intervals of rotation about the indicated carbon–carbon bonds.

The results of these calculations are given in Table 1. In both cases the results obtained using the AM1 Hamiltonian²⁰ gave conformational energy minima to structures very similar to published crystal structures²¹, while Modified Neglect of Differential Orbital (MNDO)^{14,18} calculations yielded less reasonable results. (The present study utilized the AM1 method exclusively.) The values noted as ‘two bonds’ are the energies required for rotating both phenyl units about the heterocycle (a

‘paddle-wheel’ motion of the heterocycle) and should be divided by two for comparison with the ‘one bond’ values.

The present study differs from previous work in two ways. First, our model compounds have the phenyl group as the central unit rather than the heterocycle as the central unit. For a non-substituted polymer, this should make no difference in the results relative to earlier studies. However, substituents on the phenylene rings can be modelled in a more straightforward manner with the present structures (in addition to minimizing the end effects). Second, we have gone beyond earlier work^{19,20} by systematically examining the energetic, conformational and electronic consequences at the molecular level of simple chemical substitutions.

Figure 2 shows the basic structure used to model rigid rod polymers in this study. (The arrows in the figure indicate the ‘paddle-wheel’ motion of the phenyl group.) It differs from the structures already studied in that only one heterocyclic ring is fused to benzene. Studies on previously reported structures 1A^{18,19} and 1B^{13,14} included the variations where the heteroatoms were located both *cis* and *trans* to one another. The same

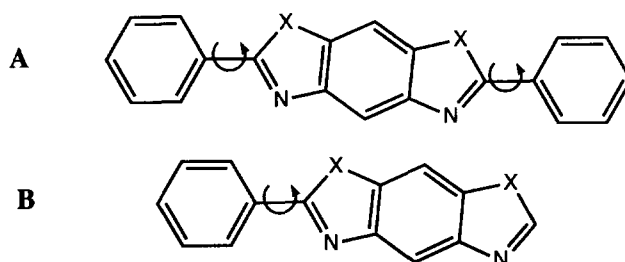


Figure 1 Model compounds used in previous studies (X=O, S, NH) (hereafter structures 1A and 1B, respectively); both *cis* and *trans* arrangements of X were considered

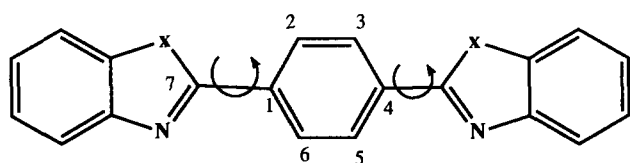


Figure 2 General model compound structure and numbering system used in this study

Table 1 AM1 calculations of rigid rod polymer models

Compound	Torsion angle (deg)		Barrier (kcal mol ⁻¹)	Ref.
	Min energy	Max energy		
	0	90	5.22 (two bonds)	19
	21	90	2.17 (two bonds)	19
	0	90	2.52 (one bond)	14
	32	90	1.23 (one bond)	14
	29	90	0.74 (one bond)	14

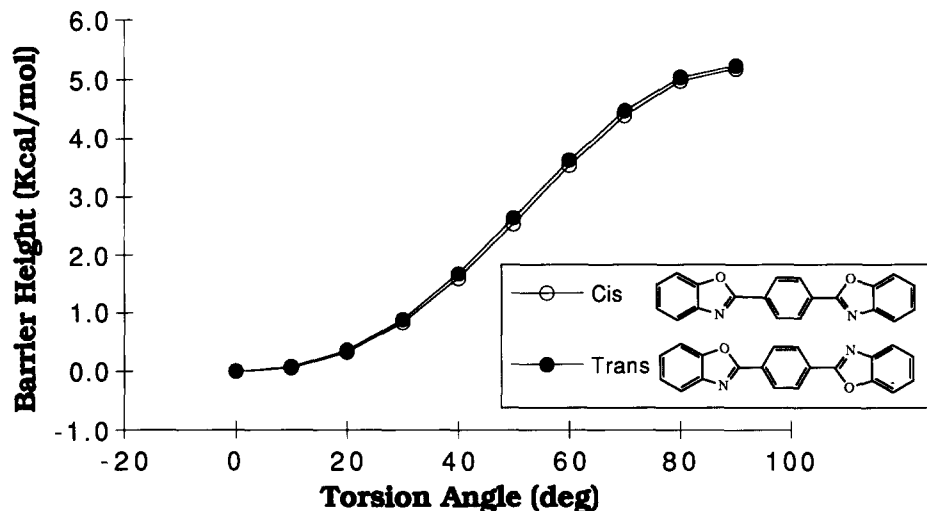


Figure 3 Conformation energy curves for *cis* and *trans* PBO model structures

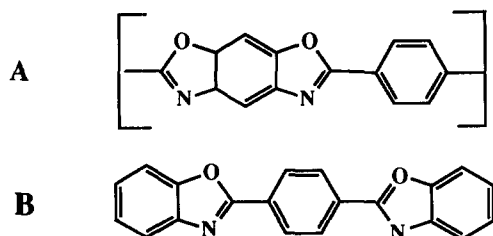


Figure 4 A, repeating unit in PBO; B, model PBO structure used in this study

variation has been provided in this study by rotating one heterocyclic system 180° with respect to the other one at the start of the calculation. As with previous calculations, the results obtained with the heteroatoms *cis* and *trans* to one another differed by less than $0.3 \text{ kcal mol}^{-1}$ in all cases. After Figure 3 we have displayed the results for the *cisoid* conformations since this simplifies the graphical representation of the calculations without diminishing their merit.

Figure 3 shows the calculated conformational energies for both conformations of the unsubstituted PBO model compound. The rotational barrier (relative energy maximum) calculated for the system is $5.2 \text{ kcal mol}^{-1}$, which is the same as that calculated for the *cisoid* structure for the other three-segment PBO model compound shown in Figure 1^{18,19}.

A potential deficiency of our model compounds is that they do not exactly mimic the structure of the mer of the rigid rod compounds of interest. Figure 4 shows the structure of the mer in PBO as opposed to the model compound used in this study. We did one set of calculations on a 'full size' model structure to demonstrate that our smaller model structures gave the same results and thus justify the saving in computation time.

The structure of the 'full sized' model compound and the results of the barrier height calculations using it are shown in Figure 5. The barrier height and curve shape obtained with this larger model species, when normalized to zero energy, is *identical* to that obtained with the smaller PBO model structure used in the rest of this study. The fact that these two structures gave identical

results suggests that long range resonance interactions have no effect on rotational barriers.

Figure 6 shows results of torsional energy calculations on unsubstituted, monomethylated, *p*-dimethylated and *o*-dimethylated PBO model species. The maximum conformational energy for each structure is specified by the arrows in the figure. With the exception of the monomethylated structure, the symmetry of these structures allows all the conformational energy information to be obtained from the 0° -to- 90° plots shown. These results, summarized in Table 2, show the effect of methylation on the torsional barriers of these structures. Torsional barriers for the unsubstituted, monomethylated, *p*-dimethylated and *o*-dimethylated structures are 5.2 , 4.0 , 2.5 and $1.7 \text{ kcal mol}^{-1}$, respectively. Also the minimum energy conformation shifts (in the same order) from the flat structure (torsion angle = 0°) to a structure in which the torsion angle is 40° . Both of these effects show that the primary effect of methylation is to *destabilize the flat conformation*, due to steric hindrance. The first methyl group lowers the barrier height by $1.2 \text{ kcal mol}^{-1}$, indicating that the flat conformation has been destabilized by that amount. If successive methylation lowers the barrier height by $1.2 \text{ kcal mol}^{-1}$ per methyl group we would expect the barrier height for the dimethylated structures to be $2.8 \text{ kcal mol}^{-1}$. For the *para* dimethyl structure the observed value is $2.5 \text{ kcal mol}^{-1}$, which is acceptably close to the predicted value. However, the barrier height for the *o*-dimethylated structure is $1.7 \text{ kcal mol}^{-1}$. This result suggests further steric crowding by the two *ortho* methyl groups, which is borne out by a consideration of the following bond angles. The calculated C7-C1-C2 bond angle (Figure 2) is a measure of the way in which the structure accommodates the crowding due to the presence of the *o*-methyl group. At 0° torsion angle this value for the *p*-dimethyl structure is 122.4° . That is, the bond angle has increased slightly relative to the value of 120° for the unsubstituted structure due to the replacement of a hydrogen atom by a methyl group. As the torsion angle goes from 0° to 90° this angle decreases from 122.4° to 120.0° , indicating a reduction in the crowding as the phenyl group rotates away from the heterocyclic moiety. In the *o*-dimethyl structure, since there are methyl groups on either side of the C7-C1 bond,

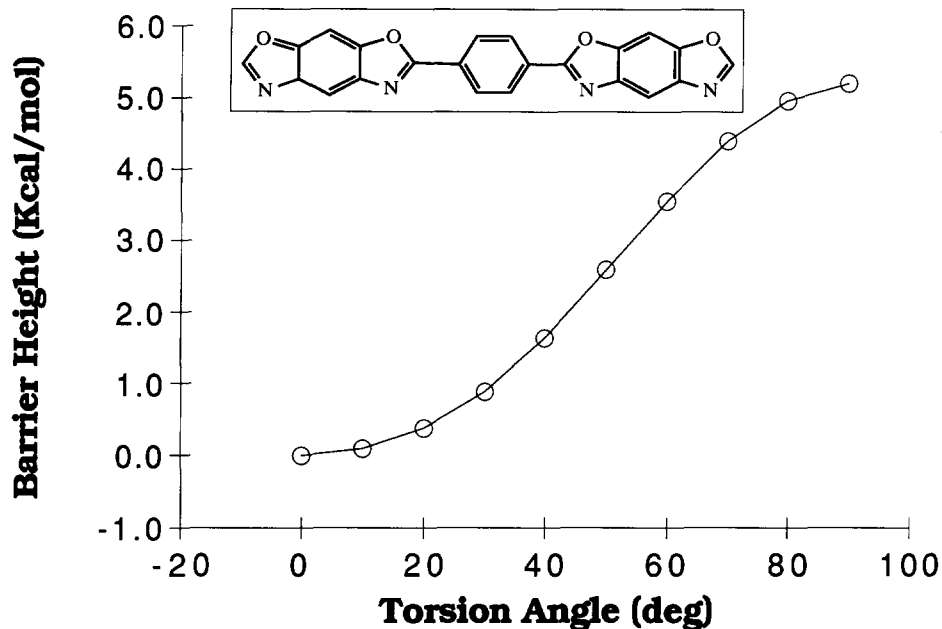


Figure 5 Conformational energy curve for large PBO model structure

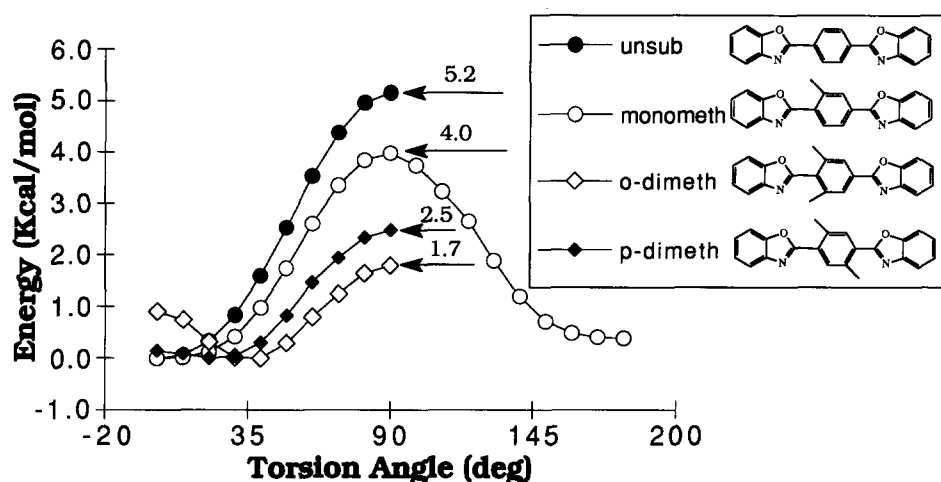


Figure 6 Conformational energy curves for unsubstituted, monomethylated, *o*-dimethylated and *p*-dimethylated PBO model structures

Table 2 Numerical summary of AM1 calculations

Structural type	Torsional angle (deg) min energy			Torsional angle (deg) max energy			Barrier (kcal mol ⁻¹)		
	X=O	X=NH	X=S	X=O	X=NH	X=S	X=O	X=NH	X=S
	0	30	10	90	90	90	5.2	2.7	2.2
	0	140	30	90	180	90	4.0	3.1	1.3
	40	50	70	90	0	0	1.7	7.1	1.7
	20	50	90	90	0	0	2.5	4.7	0.2

this bond angle is a constant 120° , regardless of the torsion angle. Thus, for the *o*-dimethylated structure, the flat conformation is additionally destabilized since the C7-C1-C2 bond angle cannot expand (relax) to accommodate the presence of one methyl group due to the presence of the other *ortho* methyl group.

Figure 7 shows results of torsional energy calculations on unsubstituted, monomethylated, *p*-dimethylated and *o*-dimethylated PBI model species, again with the energy maxima labelled by arrows. These results, also summarized in Table 2, parallel those in Figure 6 with the added factor of the steric effect of the

imidazole NH group. The difference between the imidazole N atom and the NH group requires that calculated conformation energy results be displayed from 0° to 180° for the monomethylated structure. The unsubstituted structure shows a shallow minimum at torsion angle 30° (compare with the value of 32° obtained in an earlier AM1 calculation¹⁴) with an energy maximum of $2.7 \text{ kcal mol}^{-1}$ (compare with $2.5 \text{ kcal mol}^{-1}$, ref. 14). Since the 0° conformation has two $\text{NH}\cdots\text{H}$ contacts, the flat conformation is destabilized, causing the minimum energy conformation to move away from 0° torsion angle. The 90° conformation has no $\text{NH}\cdots\text{H}$ contacts, therefore

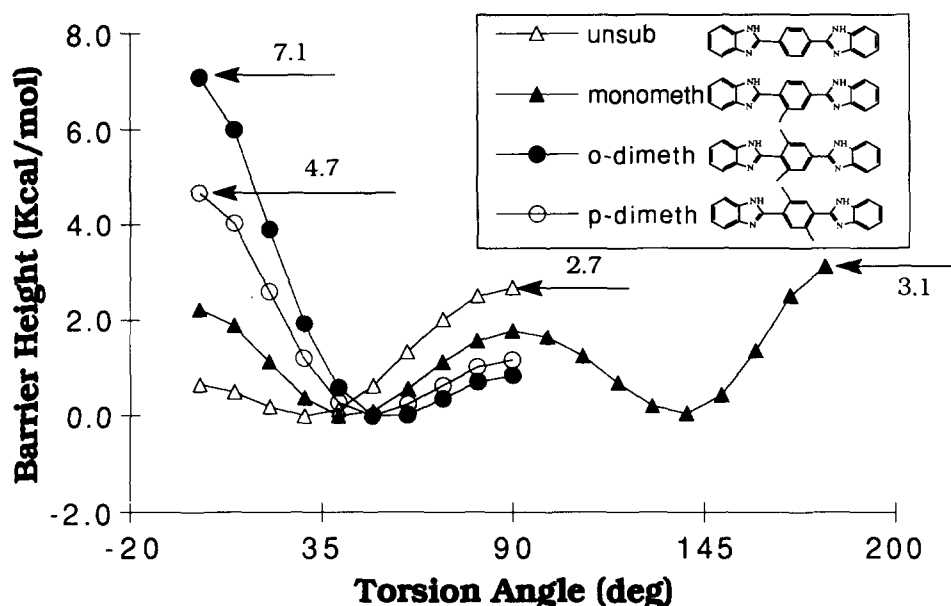


Figure 7 Conformational energy curves for unsubstituted, monomethylated, *o*-dimethylated and *p*-dimethylated PBI model structures

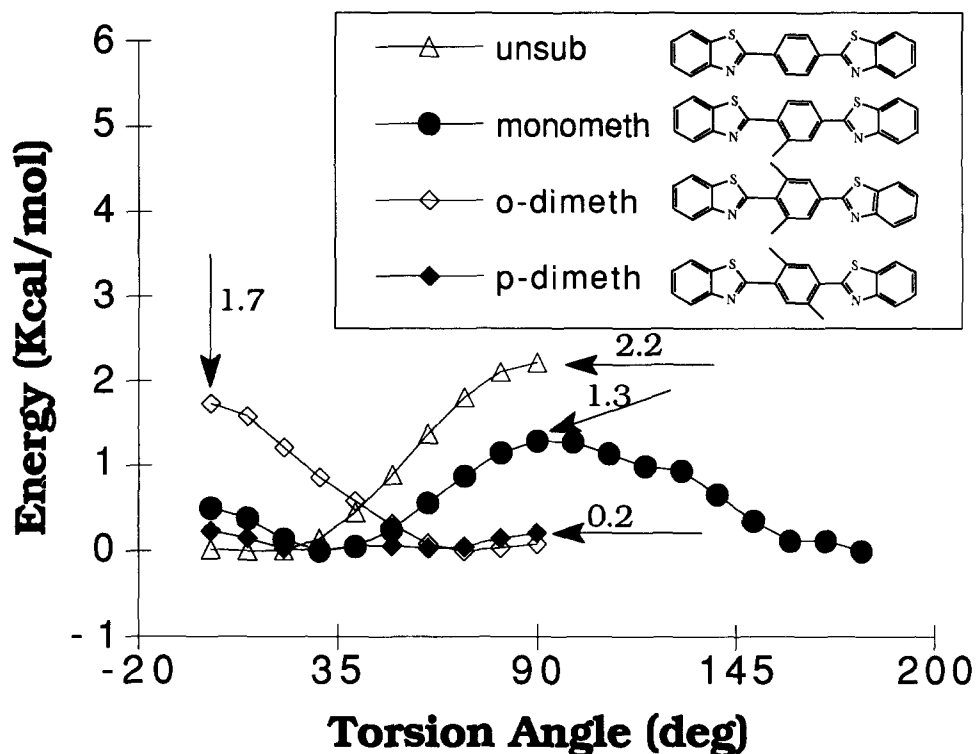


Figure 8 Conformational energy curves for unsubstituted, monomethylated, *o*-dimethylated and *p*-dimethylated PBZT model structures

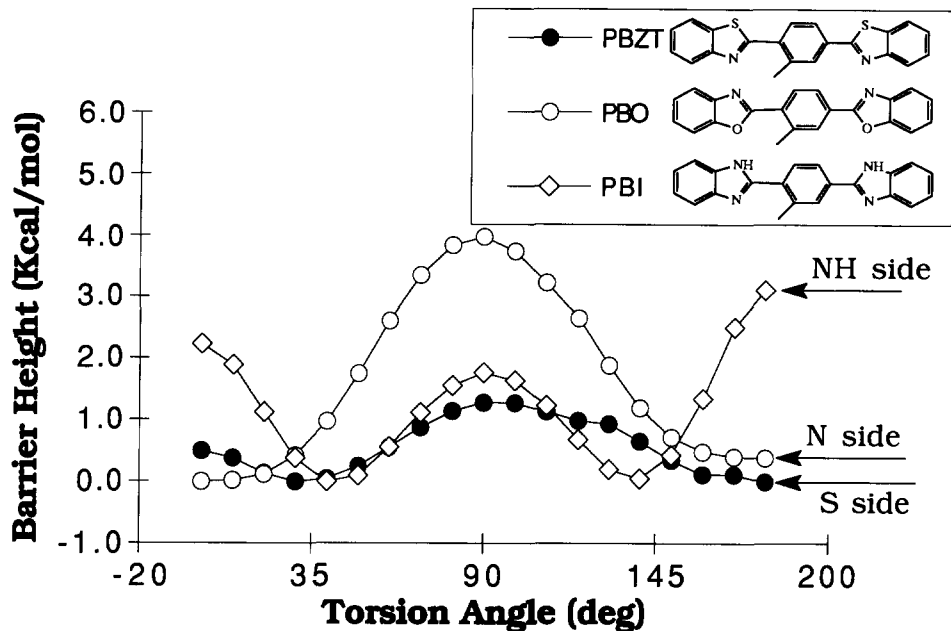


Figure 9 Conformational energy curves for monomethylated PBO, PBI and PBZT model structures

the maximum energy conformation energy is not destabilized due to steric effects, and the resulting torsional barrier is decreased compared with that of the PBO model structure. Methylation causes increased destabilization of the 0° torsion angle structures. For the monomethylated structure, the 0° torsion angle structures and the 90° torsion angle structures have nearly the same calculated energy. Additional methylation causes the 0° torsion angle structures to be higher in energy than the 90° torsion angle structures. We have been unable to analyse the results of our calculations on either unsubstituted or substituted PBI model structures in terms of simple partitioning between resonance and steric effects as shown above for PBO model species. Qualitatively, however, the two series of calculations parallel one another and the fact that the curves for the *p*-dimethylated and *o*-dimethylated structures are not superimposable again demonstrates that there is additional steric crowding in the *ortho* dimethylated structure.

Figure 8 shows the results of calculations on model PBZT compounds. The conformation energy profile for the unsubstituted species is identical to results reported by Welsh¹⁹ using the most recent sulfur parameters. The difference between the thiazole N atom and S atom requires that calculated conformation energy results be displayed from 0° to 180° for the monomethylated structure. Figure 9 is a plot of barrier height versus torsion angle for the three monomethylated structures we have studied. The 0° torsion angle is indicated in the inset in the figure for each structure. For the PBO structure the conformational energy at 180° torsion angle is slightly higher than at 0° , indicating that the nitrogen atom repels the methyl group slightly more than does the oxygen atom in this structure. The curve for the PBI structure shows the overall flattening due to steric destabilization mentioned above; also the 180° torsion angle structure is slightly higher in energy than the 0° torsion angle structure, which reflects the greater steric requirement of the NH group over the N atom. For the PBZT structure, despite the fact that the sulfur atom is larger than the

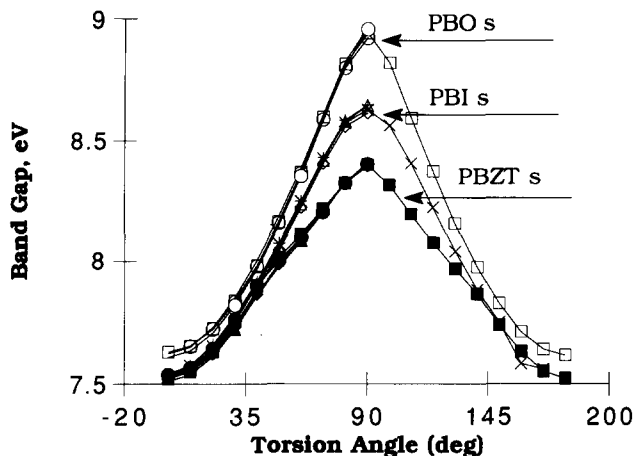


Figure 10 Band gap versus torsion angle for all PBO, PBI and PBZT model structures studied here

nitrogen atom these calculations indicate that the nitrogen atom repels the methyl group very slightly more than does the sulfur. This reflects the greater polarizability of the third row sulfur atom, which is also demonstrated in the more gradual slope of the energy curve on the sulfur side of the diagram.

Band gap versus torsion angle

The calculated band gap energy, E_g (the difference between highest occupied molecular orbital (HOMO) and lowest unoccupied molecular orbital (LUMO) energies in the model compound), is plotted versus torsion angle in Figure 10 for all the *cisoid* structures studied here. All E_g values increase monotonically as the internal phenyl group in the structure rotates away from the plane of the two heterocyclic moieties. This is a consequence of the fact that the HOMO energy decreases and the LUMO energy increases as the torsion angle tends towards 90° , as shown by the data listed in Table 3. These trends can be understood from the HOMO and LUMO plots in

Table 3 AM1-calculated band gap, HOMO energies and LUMO energies (eV) versus torsion angle for PBO, PBI and PBZT model structures

	Oxazoles (this work)	Oxazole (ref. 19)	Imidazoles (this work)	Thiazoles (this work)	Thiazole (ref. 19)
<i>Band gap values</i>					
Torsion angle = 0 deg	7.653	7.882	7.528	7.538	7.518
= 90 deg	8.924	8.626	8.615	8.403	7.758
Difference	1.270	0.744	1.086	0.865	0.24
<i>HOMO values</i>					
Torsion angle = 0 deg	-8.913	-8.863	-8.527	-8.801	-8.516
= 90 deg	-9.444	-9.252	-9.009	-8.977	-8.544
Difference	-0.531	-0.39	-0.482	-0.176	-0.028
<i>LUMO values</i>					
Torsion angle = 0 deg	-1.25	-0.981	-0.998	-1.263	-0.999
= 90 deg	-0.520	-0.624	-0.394	-0.574	-0.786
Difference	0.74	0.35	0.60	0.69	0.21

Figure 11 (frontier orbital plots for PBI and PBZT were similar). The HOMO is π antibonding across the C7-C1 bond and rotation about this bond decreases the antibonding interaction, which, of course, stabilizes the orbital. The LUMO is π bonding across the C7-C1 bond and rotation about the bond decreases the bonding interaction, destabilizing the orbital.

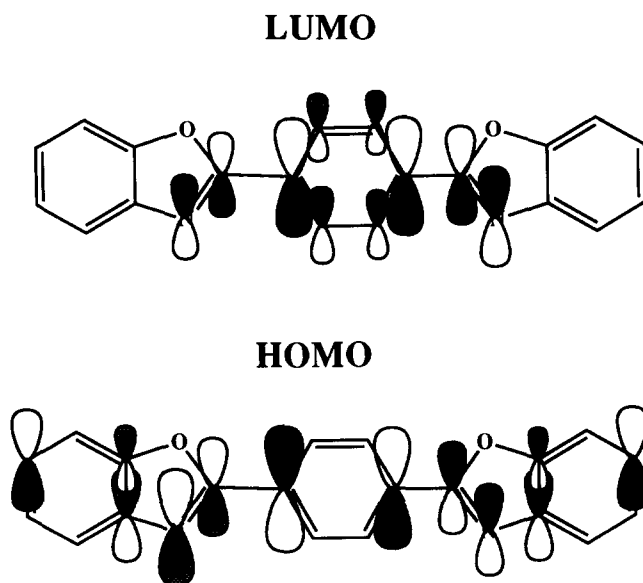
The nature of the heteroatom affects the numerical value of E_g , i.e. oxazole > imidazole > thiazole. Methylation of the phenyl group has no effect on the calculated E_g . It is obvious from a comparison of these results with those previously reported¹⁹ (Table 3) that the absolute value of the band gaps is quite model-dependent. Previous model structures gave the same trends as we observe here but the overall band gap differences reported are much smaller than we calculate, especially in the case of the thiazole structure. This is reasonable since the central unit of the earlier model is the three fused ring heterocycle. This has more π -orbitals (and a greater extent of delocalization within the central ring) contributing to it than the phenylene unit in our models. Rotation of the capping groups will be less of a perturbation (in a relative sense) for the heterocyclic ring in the central position, and hence will cause a smaller shift in the band gap. The relevance of these shifts to larger, more delocalized systems is thus unclear at present.

NLO properties versus torsion angle

The mathematical description of the dipole moment, μ , of a molecular substance in the presence of an electrical field is given by the equation:

$$\mu_i(E) = \mu_0 + \sum_j \alpha_{ij} E_j + \sum_{jk} \beta_{ijk} E_j E_k + \sum_{jkl} \gamma_{ijkl} E_j E_k E_l$$

i.e. the total molecular dipole moment is the sum of the permanent dipole moment (μ_0) and the polarizability (α) times the first power of the electric field (E), plus two additional terms which reflect the nonlinear response of the substance to the electric field²². The coefficients β and γ are referred to as the first- and second-order hyperpolarizabilities, respectively. The coefficient γ is calculated in the MOPAC package as the fourth derivative of the energy of the molecule, as represented by the heat of formation, with respect to the electric field strength. (This calculation is considered more reliable than the equivalent third derivative of the dipole moment with respect to electric field strength.) The average value

**Figure 11** Frontier orbital plots for PBO

of γ reported is a weighted average of the appropriate tensor component values.

Figure 12 shows a plot of $1/6\text{th}^*$ of the calculated average second-order hyperpolarizabilities versus torsion angle for the PBO and *o*-dimethylated PBO model structure used in this study. The experimental second-order hyperpolarizabilities of PBO and PBZT mentioned above are bulk properties while γ is the underlying molecular property. The mathematical relationship between these two quantities requires a detailed knowledge of the structure of the polymer film²³.

The main feature shown in Figure 12 is that γ decreases by a factor of about five as the torsion angle varies from 0° to 90° on both structures investigated. There is a small effect on the calculated absolute value of γ due to *o*-dimethylation (we chose to compare the unsubstituted structure with the *o*-dimethylated one because they show the greatest difference in conformational properties), but

* Documentation provided with the MOPAC program package indicates that the calculated values of γ should be divided by six to conform to experimental convention

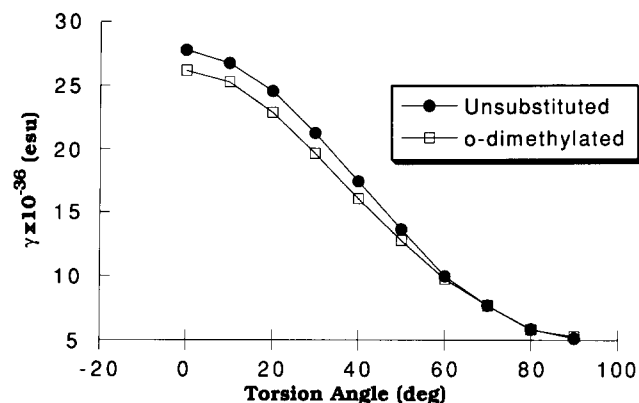


Figure 12 Second hyperpolarizabilities versus torsion angle for unsubstituted and *o*-dimethylated PBO model structures

the shape of the curve is not altered. Since γ is primarily due to the ease of internal flow of the π electrons through the molecular structure²⁴, it is not surprising that alteration of the molecular conformation in such a way as to reduce conjugation reduces the value of γ , nor is it surprising that this effect is not sensitive to methylation of the polymer backbone, since methylation has little or no effect on conjugation.

The data plotted in Figures 6–8 above show that methylation of the phenyl group in these model structures has the general effect of destabilizing the flat structures due to steric interactions. While we have made no attempt to model interchain interactions, this suggests that polymers substituted in this way may deviate significantly from the flat conformation. Such deviation would, according to our calculations, result in a decrease in desirable NLO effects.

CONCLUSIONS

The calculated torsional barriers obtained using the structure shown in Figure 2 are in excellent agreement with literature values for other PBO, PBI and PBZT model structures. Further calculations showed that the effect of phenyl methylation is to reduce torsional barriers in all cases, due to steric destabilization of the flat conformation.

Calculation of electronic band gaps and second-order hyperpolarizabilities, both of which depend on π electron delocalization, show the same effect of decrease in π electron delocalization as the torsion angle increases. Consequently the band gap increases with torsion angle while the second-order hyperpolarizability decreases. Methylation of the phenyl group has essentially no effect on either of these quantities. However, since substitution changes the minimum in the torsion potential, the opto-electronic factors can be influenced (generally decreased) in a secondary sense in that substitution pushes the structures away from planarity.

The trends in torsional effects on band gaps is consistent with recently published results¹⁹. However, the model dependence of the results indicates significantly larger model compounds or infinite systems (periodic boundary conditions) should be employed to obtain quantitatively meaningful results. This work is in progress.

ACKNOWLEDGEMENTS

This work was initiated during the USAF–UES Summer Faculty Research Program (Contract F49620-88-C-0053). JWC gratefully acknowledges the opportunity to participate in this program; he also gratefully acknowledges helpful conversations with Professor A. H. Holder, Chemistry Department, University of Missouri–Kansas City.

REFERENCES

- 1 Wolfe, J. F. and Arnold, F. E. *Macromolecules* 1981, **14**, 909
- 2 Wolfe, J. F., Bock, H. L. and Arnold, F. E. *Macromolecules* 1981, **14**, 915
- 3 Choe, E. W. and Sang, N. K. *Macromolecules* 1981, **14**, 920
- 4 Evers, R. C., Arnold, F. E. and Helminiak, T. E. *Macromolecules* 1981, **14**, 925
- 5 Allen, S. R., Fillipov, A. G., Farris, R. J., Thomas, E. L., Wong, C.-P., Berry, G. C. and Chenevey, E. C. *Macromolecules* 1981, **14**, 1135
- 6 Kumar, S. and Helminiak, T. E. *Mater. Res. Soc. Meeting Abstr.* Fall 1988, p. 307
- 7 Hunsaker-Jubara, M. Masters Thesis, Wright State University, 1982
- 8 Feast, W. J. in 'Handbook of Conducting Polymers' (Ed. T. A. Skotheim), Vol. 1, Marcel Dekker, New York, 1986, pp. 1–43
- 9 Prasad, P. N. and Williams, D. J. 'Introduction to Nonlinear Optical Effects in Molecules and Polymers', Wiley-Interscience, New York, 1991, p. 241
- 10 Prasad, P. N. and Williams, D. J. 'Introduction to Nonlinear Optical Effects in Molecules and Polymers', Wiley-Interscience, New York, 1991, pp. 42–54
- 11 Tsai, T. T. and Arnold, F. E. *Polym. Prepr.* 1986, **27** (2), 221
- 12 Burkette, J. and Arnold, F. E. *Polym. Prepr.* 1987, **28** (2), 278
- 13 Tsai, T. T. and Arnold, F. E. *Polym. Prepr.* 1987, **29** (2), 324
- 14 Farmer, B. L., Wiershke, S. G. and Adams, W. W. *Polymer* 1990, **31**, 1637
- 15 Quantum Chemistry Program Exchange, Indiana University, Bloomington, IN 47405, No. 506
- 16 Dewar, M. J. S. and Yuan, Y.-C. *Inorg. Chem.* 1990, **29**, 3881
- 17 Quantum Chemistry Program Exchange, Indiana University, Bloomington, IN 47405, No. 455
- 18 Yang, Y. and Welsh, W. J. *Macromolecules* 1990, **23**, 2410
- 19 Welsh, W. J. and Yang, Y. *Comp. Polym. Sci.* 1991, **1**, 139
- 20 Dewar, M. J. S., Zoebisch, E. G., Healy, E. F. and Stewart, J. J. D. *J. Am. Chem. Soc.* 1985, **107**, 3902
- 21 Wellman, M. W., Adams, W. W., Wolff, R. A., Dudis, D. S. and Fratini, A. V. *Macromolecules* 1981, **14**, 935
- 22 Prasad, P. N. and Williams, D. J. 'Introduction to Nonlinear Optical Effects in Molecules and Polymers', Wiley-Interscience, New York, 1991, p. 36
- 23 Prasad, P. N. and Williams, D. J. 'Introduction to Nonlinear Optical Effects in Molecules and Polymers', Wiley-Interscience, New York, 1991, pp. 59–80
- 24 Welsh, W. J. and Mark, J. E. in 'Molecular Level Calculations of the Structure and Properties of Non Crystalline Polymers' (Ed. J. Bicerano), Wiley, New York, in press